COPAS Annual Report
Altimetry High-Latitude Performance

Reference: CLS-ENV-RP-22-0474

Issue: 2.0

Date: October 25, 2023

Contract: COPAS_460000262

Costumer:	EUMETSAT	**Document Ref.:**	CLS-ENV-RP-22-0474
Contract No.:	COPAS_460000262	**Date:**	October 25, 2023
		Issue	2.0

Project:	COPERNICUS ALTIMETRY SERVICE FOR THE SENTINEL-3 MISSION		
Title:	COPAS Annual Report Altimetry High-Latitude Performance		
Author(s):	P. Prandi, Mission Performance Team Head, CLS		
Approved by:	F. Nencioli COPAS Coordinator, CLS	**Authorized by:**	Sylvie Labroue Technical Performance Manager, CLS
Distribution	EUMETSAT		
Accepted by EUMETSAT	C. Nogueira Loddo Technical Officer, EUMETSAT		
Filename:	CLS-ENV-RP-22-0474.pdf		

Change Log

Version	Date	Changes
1.0	July, 29, 2023	First Draft
2.0	October 25, 2023	First revision

Table of Content

List of Figures

1 Introduction

This report synthetizes the analysis of the performance of Sentinel-3A and 3B missions over polar oceans for year 2023. It aims to complement NTC cyclic reports provided in the frame of the COPAS contract with a longer-term perspective on the evolution of sea level in polar oceans. It also provides comparisons to other satellite radar altimetry missions in polar regions.

Note that the analysis performed here is focused on **polar ocean** sea surface height variability. It does not adress any cryospheric variables (such as sea-ice freeboard for example).

The report is structured in 4 chapters (excluding this introduction):

chapter 2 describes the datasets and preprocessing used in this report,

chapter 3 provides an overview of Sentinel-3 missions over polar oceans,

chapter 4 provides comparisons between Sentinel-3 and other altimetry missions,

chapter 5 provides a validation of polar ocean with respect to insitu measurements.

2 Data and processing description

This chapter of the report describes the data and pre-processing used to perform the analysis presented in the current report.

2.1. Input products

This section describes the input satellite altimetry data used in this analysis.

2.1.1. Sentinel-3

All Sentinel-3 data used in the present analyis originate from PDGS Marine Level-2 products. Processing Baselines used over the period of analysis are summarized in table 1. The analysis in this report is based on the latest Sentinel-3 reprocessing campaign which provides an homogeneous processing over the full time span.

mission	from	to	PB reference
Sentinel-3A	February 2016	April 2023	SR_WAT_005.02
Sentinel-3B	April 2018	April 2023	SR_WAT_005.02

Table 1: Sentinel-3 processing baselines used in this report

Unless stated otherwise, we rely on product variables available in PDGS Level 2 NTC products. The product variables used in this analysis are summarized in table 2.

physical quantity	product variable
SSHA over sea ice	sea_ice_ssha_20_ku
SSHA over ocean	ssha_20_ku
lead/ocean flag	surf_type_flag_20_ku

Table 2: Sentinel-3 level 2 product variables used in this report

2.1.2. SARAL/AltiKa

SARAL/AltiKa GDR-F data is used in this report, a description of the content and perfomance of this processing baseline is available in [3]. The Adaptive retracker is used, as well as the neural network echo shape classification to separate leads and ocean. Additionnal editing criteria are used to select valid measurements, the editing procedure is described in [5]. This dataset was used by [5] and [1] to build multi-mission topography maps of the ice-covered Arctic and Southern oceans respectively.

2.1.3. CryoSat-2

CryoSat-2 provides polar ocean observations up to 88°N thanks to its high inclination orbit. In this report we use Cryo-TEMPO Polar Ocean data. This thematic dataset provides along-track polar ocean observations for the Arctic Ocean only. Data were downloaded from http://cryosat.mssl.ucl.ac.uk/tempo/. The Cryo-TEMPO product handbook can be donwloaded from http://cryosat.mssl.ucl.ac.uk/tempo/public-docs.html. Data processing details are available in an ATBD from https://earth.esa.int/documents/20142/37627/Cryo-TEMPO-ATBD-Polar-Oceans.pdf/8457bd6e-34c7-571e-561b-c5e533b4f83a.

2.1.4. In-situ

Two in-situ stations are used in this report to validate SSHA retrievals in polar oceans (see chapter **5**), one in the Arctic Ocean and one in the Southern Ocean.

In the Arctic Ocean, recordings from a BPR deployed à 75°N and 210°E in the frame of the BGEP program (https://www2.whoi.edu/site/beaufortgyre/) are used. The dataset can be retrieved from https://www2.whoi.edu/site/beaufortgyre/data/mooring-data/.

In the Southern Ocean, we use SSH measurements from a Japanese tide gauge at Syowa (https://www.sonel.org/spip.php?page=maregraphe&idStation=2000). Tide gauge measurements were downloaded from the Univesity of Hawai'i Sea Level Center. The UHSLC provides different ways to access the data, they can be found at https://uhslc.soest.hawaii.edu/data/?rq.

3 Polar ocean sea level variability from Sentinel-3 mission

This section provides a synthetic view of polar ocean sea level variability as observed by the Sentinel-3 mission. The content is mainly similar to what is available in cyclic reports, but with a different perspective based on the analysis of longer time periods.

This chapter is structured in 3 parts:

1. A statiscal analysis of the distribution of leads and its evolution (section 3.1.),
2. An analysis of sea level variability in polar oceans (section 3.2.),
3. An estimation of the leads/ocean SSHA bias over a long period (section 3.3.),
4. An analysis using crossovers (section 3.4.).

3.1. Polar oceans observability

Our capability to retrieve sea surface height in ice-covered areas of polar regions (both in the Arctic and Southern oceans) is based on the accurate identification of leads in the ice pack. Leads correspond to cracks in the ice pack which form as a response to wind and ocean current stress on the floating ice. Leads act as bright targets (they generally exhibit small waves conditions) and the corresponding echoes are generally very peaky.

The goal of this first section is to compare leads detection over a long period (one year) for Sentinel-3A and Sentinel-3B in order to check the consistency between both missions.

Figures 1 and 2 display the number of leads and ocean measurements for Sentinel-3A and Sentinel-3B in the Arctic and Southern oceans, respectively. These are derived directly from the product based on the surface classification flag, all latitudes above 50°N (below 50°S) are considered.

The seasonal pattern observed on both Sentinel-3A and Sentinel-3B is consistent with the seasonal sea ice cycle: in the Arctic Ocean the number of leads detected peaks in norhern hemisphere winter when the ice extent is maximum. In the Southern Ocean, there are almost no leads detected in the southern hemisphere summer: almost all sea ice around antarctica disappears, with only small portions of the ocean still covered with ice around the Antarctic peninsula.

Figures 3 and 4 show maps of the ratio of measurements identified as leads for Sentinel-3A and Sentinel-3B in the Arctic and Southern oceans, respectively.

Figures 5 shows maps of the differences between Sentinel-3A and Sentinel-3B for the ratio of measurements identified as leads in the Arctic and Southern oceans. The consistency between both missions is excellent with differences below 5% in terms of polar ocean observability. Since Sentinel-3A and Sentinel-3B do not observe the same ocean at the same time and sea-ice dynamics, some level of discrepancy is expected.

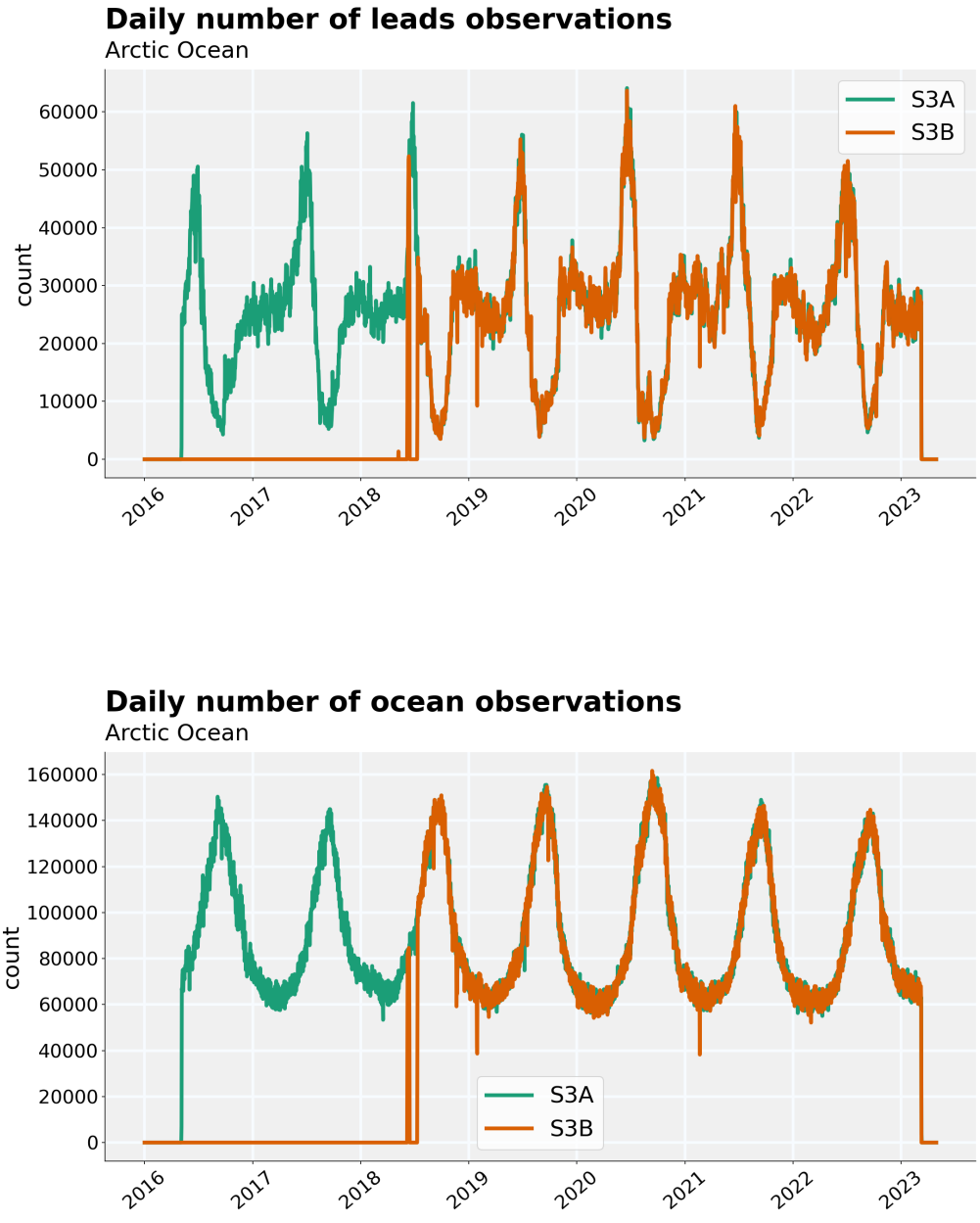

Figure 1: Number of leads and open ocean measurements in the Arctic ocean

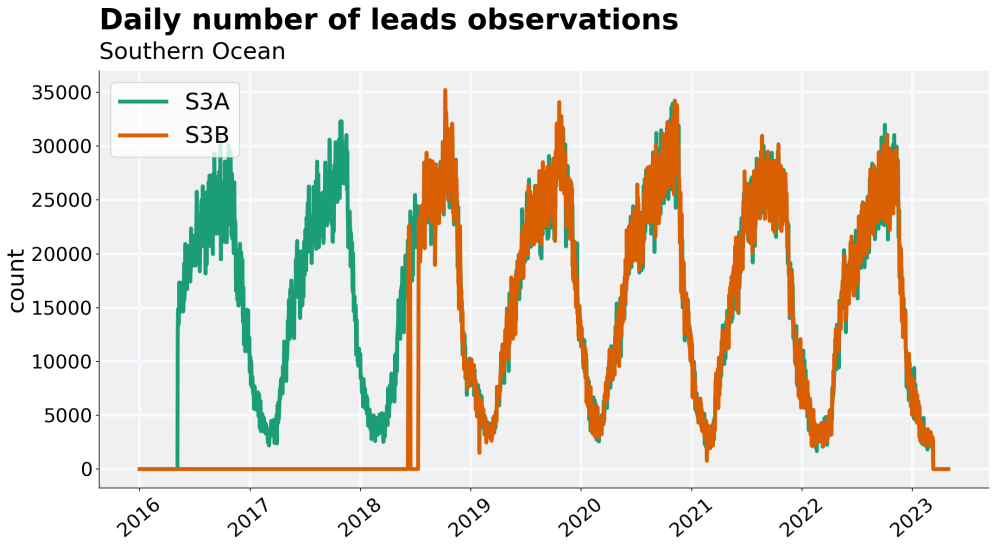

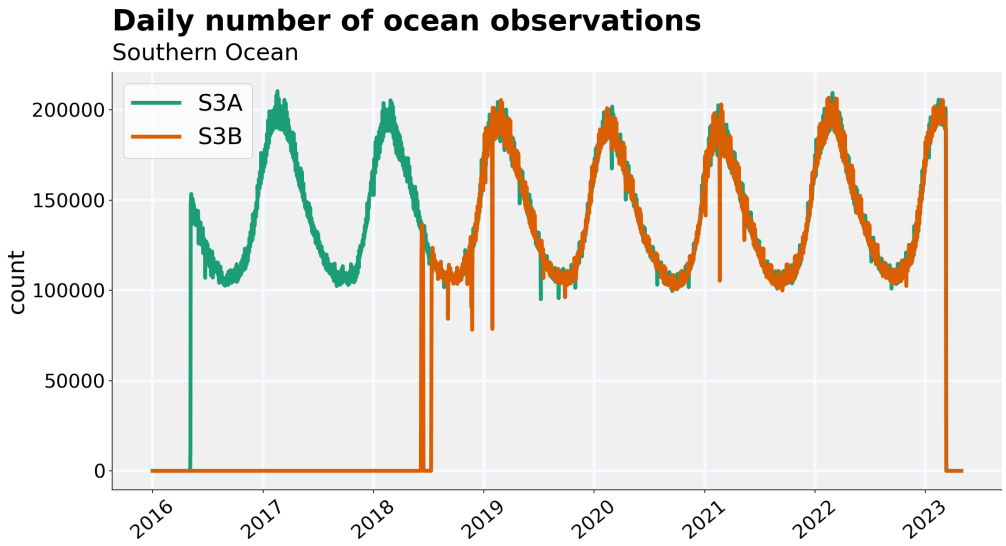

Figure 2: Number of leads and open ocean measurements in the Southern ocean

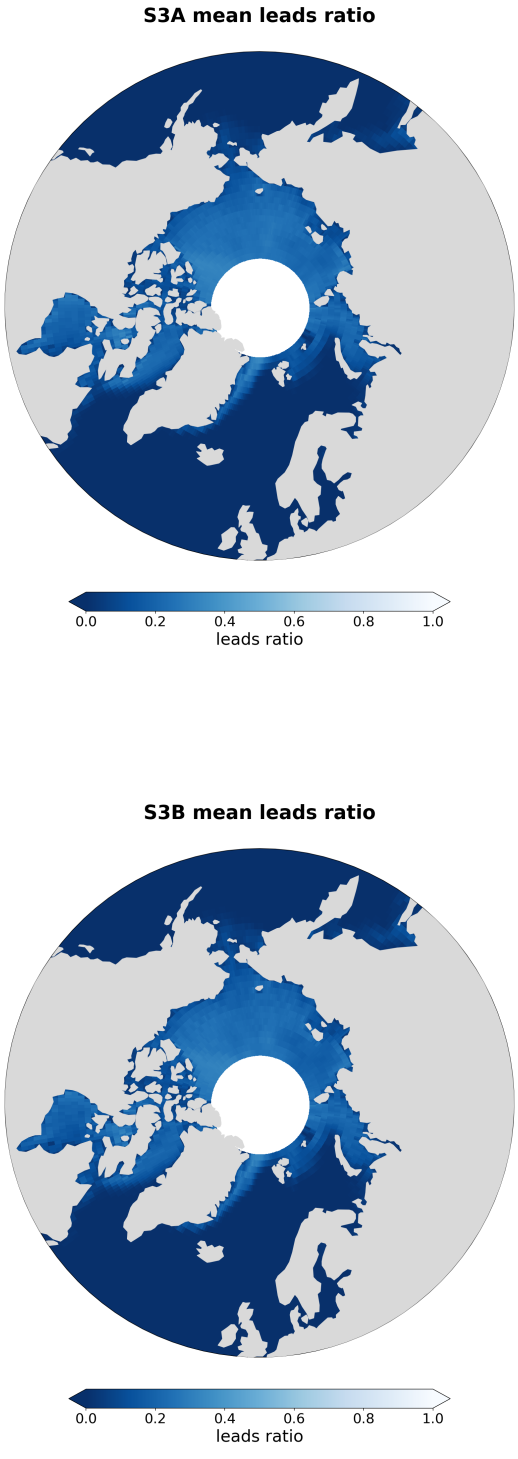

Figure 3: Ratio of measurements identified as leads for Sentinel-3A (top) and Sentinel-3B (bottom) in the Arctic Ocean

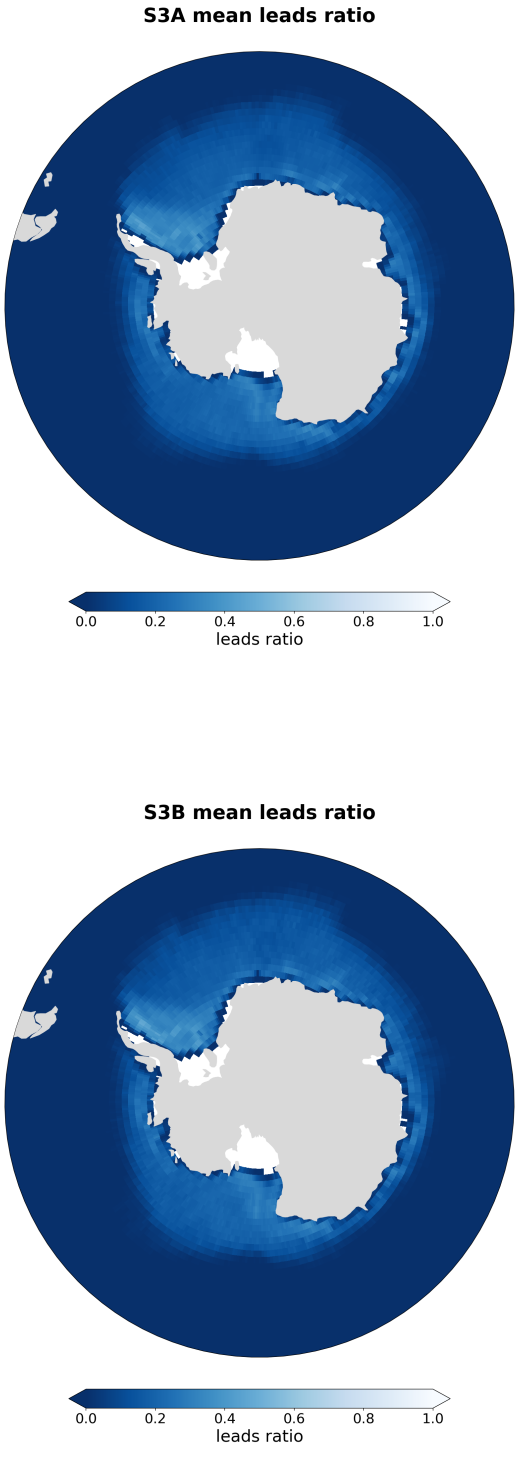

Figure 4: Ratio of measurements identified as leads for Sentinel-3A (top) and Sentinel-3B (bottom) in the Arctic Ocean

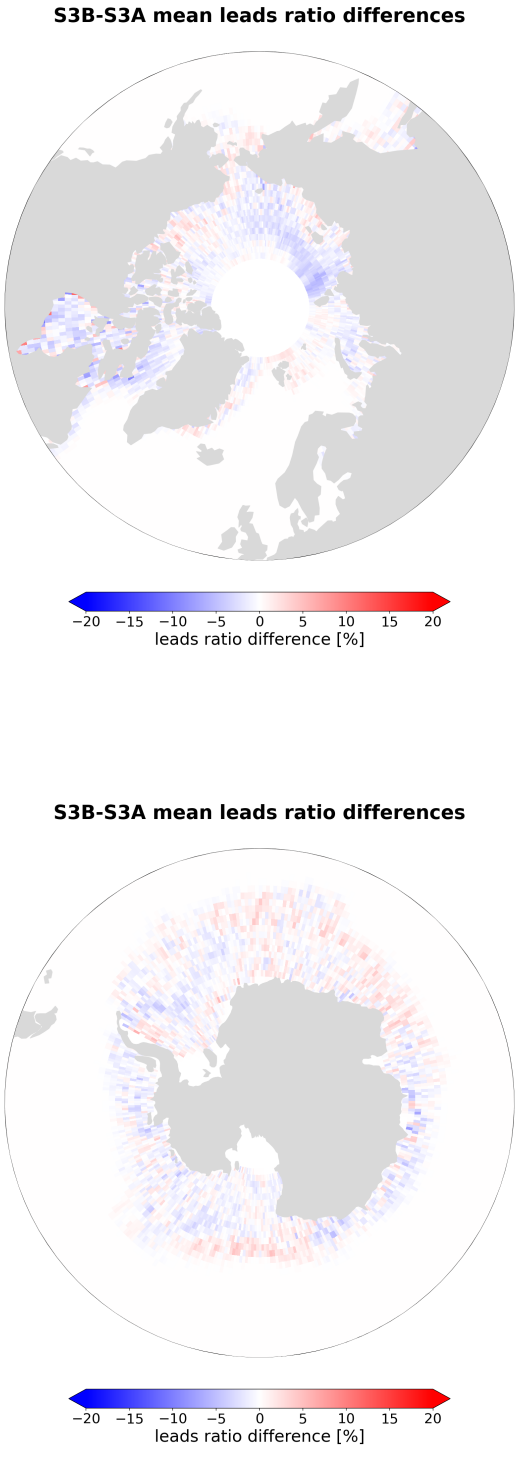

Figure 5: Differences in the ratio of leads measurements between Sentinel-3A and Sentinel-3B for the Arctic (top) and Southern (bottom) oceans

3.2. Polar sea level variability

NTC cyclic reports produced within the COPAS framework already contain some metrics about polar ocean SSHA. Here we complement these cycle per cycle analyses with a long-term point of view on the variability of polar ocean SSHA. The maps and time series presented here are estimated with any offset between the open ocean and leads empirically removed (see section 3.3.) in order to minimize artifacts originating from processing discontinuities.

3.2.1. Time variability

Figure 6 displays the timeseries of regional mean SSHA in the Arctic and Southern oceans observed for Sentinel-3A and Sentinel-3B. Both the open and ice-covered oceans are considered here. Sentinel-3A and Sentinel-3B observe the polar oceans very consistently.

This is further exhibited on figure 7, which shows the differences between Sentinel-3A and Sentinel-3B regional mean SSHA in the Arctic and Southern oceans. Daily differences remain below 2 cm, with some day to day variability, due to the different daily samplings between both orbits.

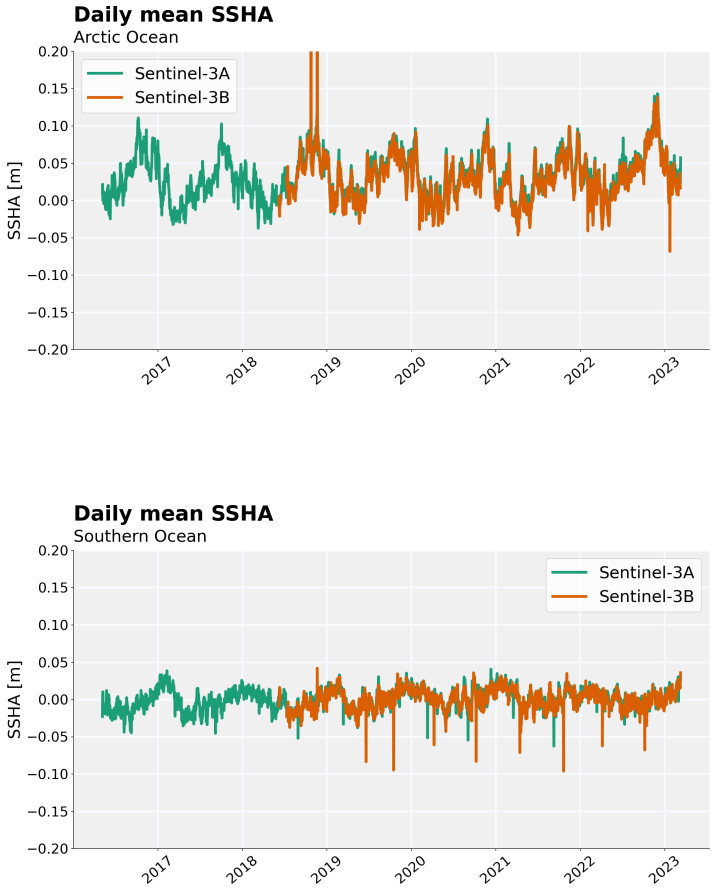

Figure 6: Regional mean SSHA in the Arctic (top) and Southern oceans (bottom) for Sentinel-3A and Sentinel-3B

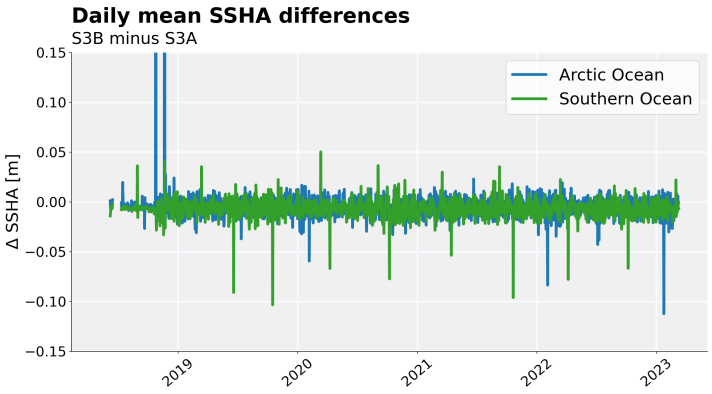

Figure 7: Regional mean SSHA differences between Sentinel-3A and Sentinel-3B in the Arctic and Southern oceans

3.2.2. Geographical variability

Figures 8 and 9 display SSHA maps for the Arctic and Southern oceans as observed by Sentinel-3A and Sentinel-3B. Each map is estimated over each missions full lifetime. The large scale patterns of polar ocean topography are captured consistently between both missions.

Figures 10 displays the maps of mean SSHA differences between Sentinel-3A and Sentinel-3B in the Arctic and Southern oceans.

Figure 11 shows the map of the standard deviation of SSHA in the Arctic Ocean for Sentinel-3A (similar behaviors are observed for Sentinel-3B and the Southern Ocean - not shown). The Arctic interior shows higher levels of SSHA variability. Natural ocean variability is not expected to be higher than at lower latitudes, this ssha variance increase can result from:

- the lack of a dedicated and finely tuned editing procedure,
- a higher noise level on range estimation from lead echoes,
- larger errors on geophysical corrections in ice-covered areas,
- a non-optimal lead detection algorithm.

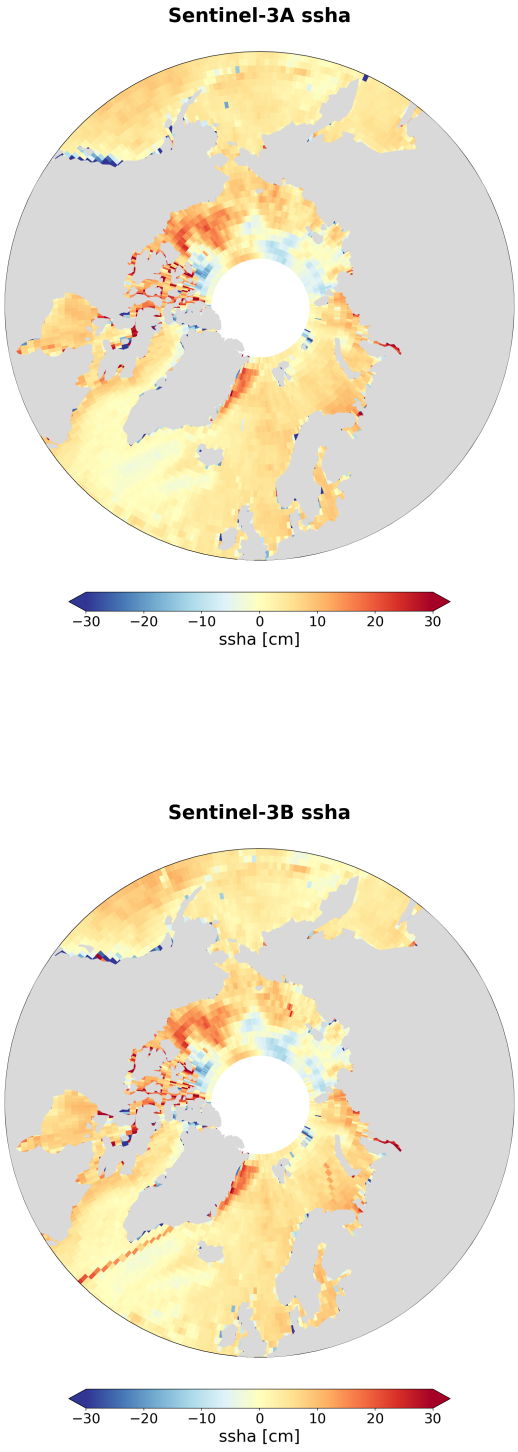

Figure 8: Maps of SSHA in the Arctic for Sentinel-3A and Sentinel-3B

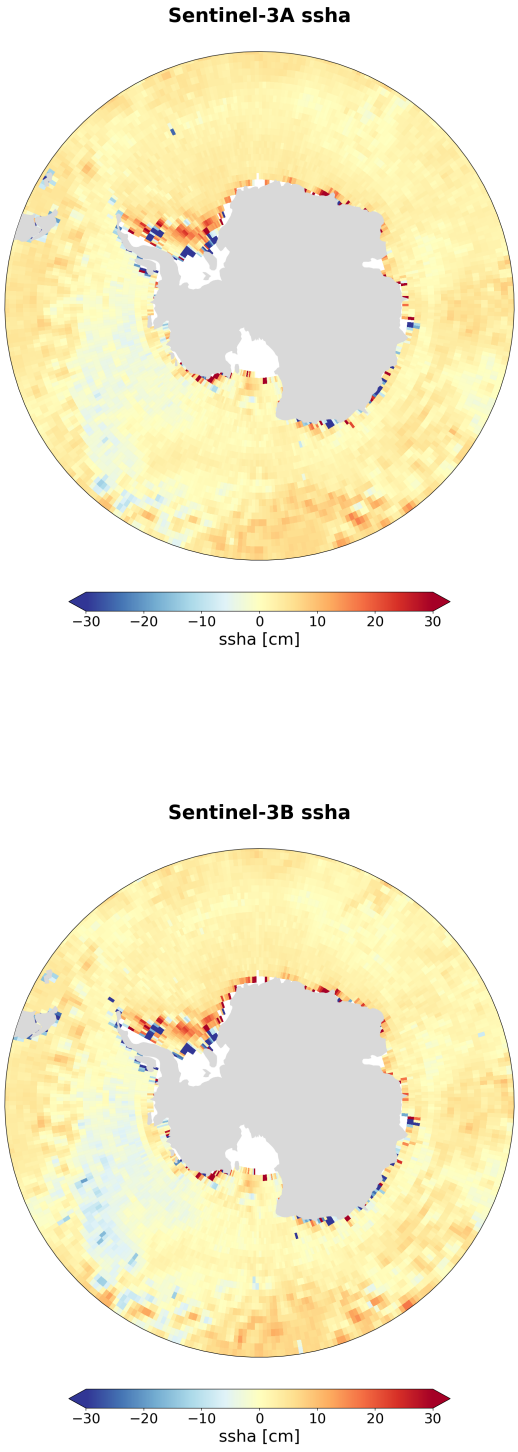

Figure 9: Maps of SSHA in the Southern ocean for Sentinel-3A and Sentinel-3B

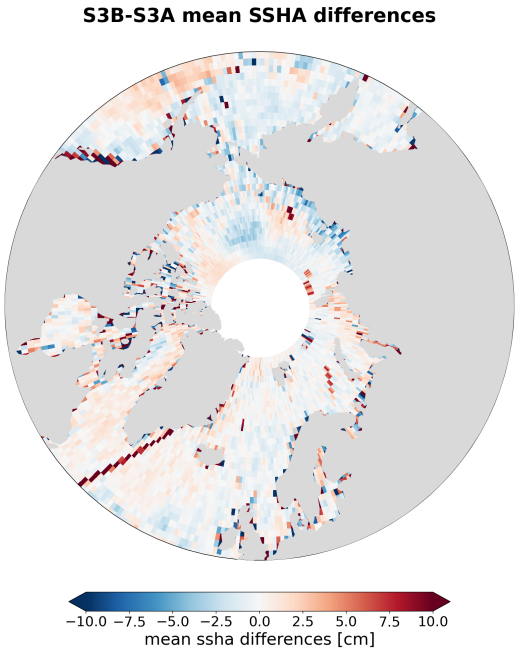

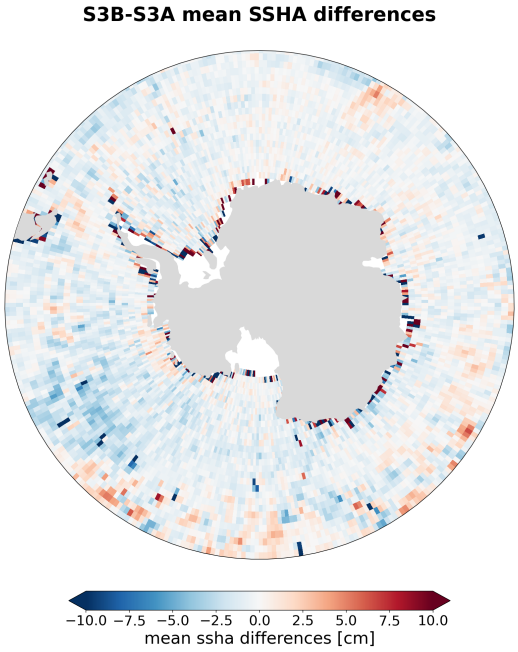

Figure 10: Maps of SSHA differences between Sentinel-3A and Sentinel-3B in the Arctic and Southern oceans

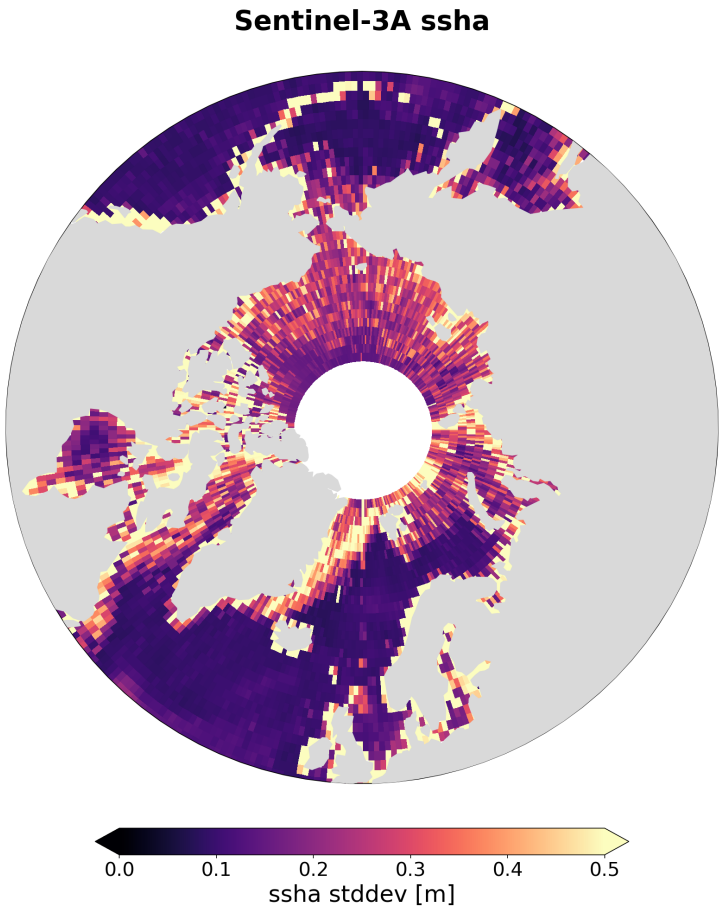

Figure 11: Map of SSHA std in the Arctic for Sentinel-3A

3.2.3. Seasonal climatology

Figure 12 provides the seasonal cycle of polar ocean SSHA in the Arctic and Southern Oceans as observed by Sentinel-3A and Sentinel-3B. Both missions show very consistent behaviors in both hemispheres. In the Southern Ocean the maximum of SSHA is reached in February, in the Arctic Ocean, the maximum is reached around November. The large spread around the mean seasonal cycle (given at 1 sigma level) results from both short term (within one month) and long term (year-to-year) SSHA variability.

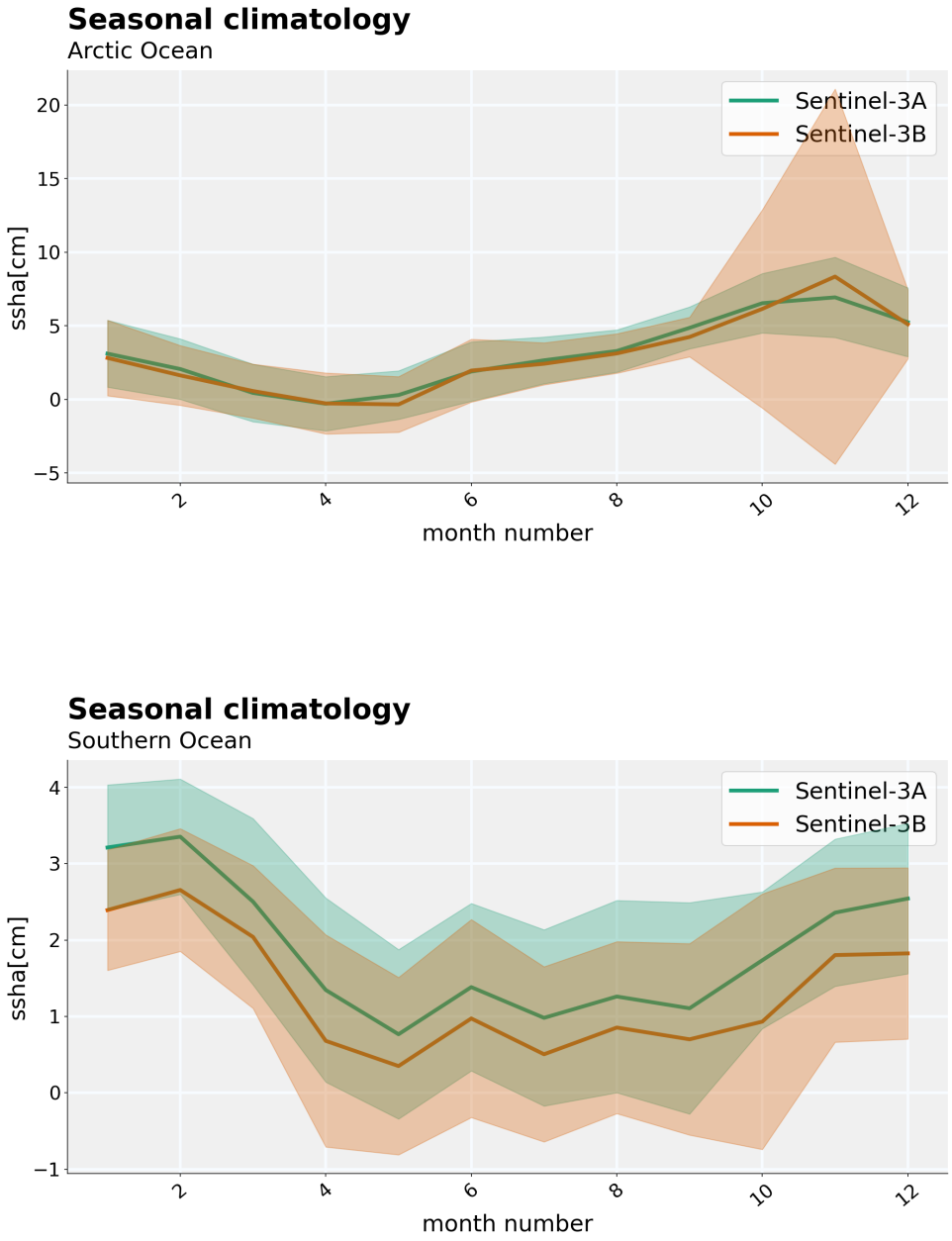

Figure 12: Seasonal SSHA climatology for Sentinel-3A and Sentinel-3B in the Arctic and Southern oceans

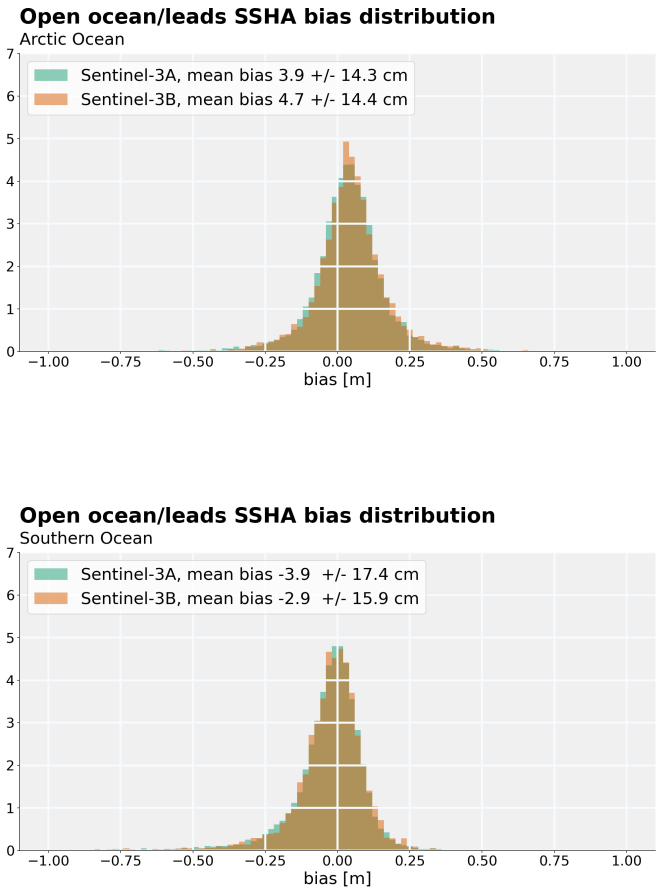

Figure 13: Distribution of open ocean/ice-covered SSHA differences for Sentinel-3A and Sentinel-3B in the Arctic and Southern oceans

3.3. Leads/open ocean bias estimation

For oceanography purposes, a key feature of a polar ocean oriented processing is the ability to provide a transition between the open and ice-covered oceans that is free of any offset between both surfaces. Any offset in SSH or SSHA will translate into a geostrophic current anomaly in downstream products, which would just be an artifact of processing inconsistencies.

Estimating any offset between open and ice-covered oceans is therefore crucial. We estimate this bias by gridding open-ocean and ice-covered SSHA measurements independently and computing the difference between both grids. Each time a grid cell has seen both open-ocean and ice-covered measurements, it provides one estimation of the inter-surface bias.

This is hard to do with a reasonable accuracy level on a cycle per cycle basis due to the low number of coincident measurements. An analysis over a longer period, as performed for this annual report provides a more reliable bias estimate.

Figures 13 displays the distribution of SSHA biases separated by mission (Sentinel-3A and Sentinel-3B) and region. The mean bias absolute values are below ≈ 5 cm, but with a large uncertainty ≈ 15 cm. Interestingly leads/ocean bias is slightly negative for the Southern Ocean and slightly positive for the Arctic

Ocean. The bias distribution on the Southern Ocean appears to slightly skewed.

There is also a geographical dependency of this bias, which is displayed on figures 14 (for the Arctic ocean) and 15 (for the Southern ocean) for both Sentinel-3A and Sentinel-3B.

In addition to geographical variability, the leads/open ocean bias also exhibits time-dependent variability, as shown on figure 16. While there is no obvious pattern in the Arctic Ocean bias, there is a clear annual signal in the Southern Ocean.

Cycle to cycle variability is large in both cases and underlines the high uncertainty levels associated to the empirical estimation of such biases.

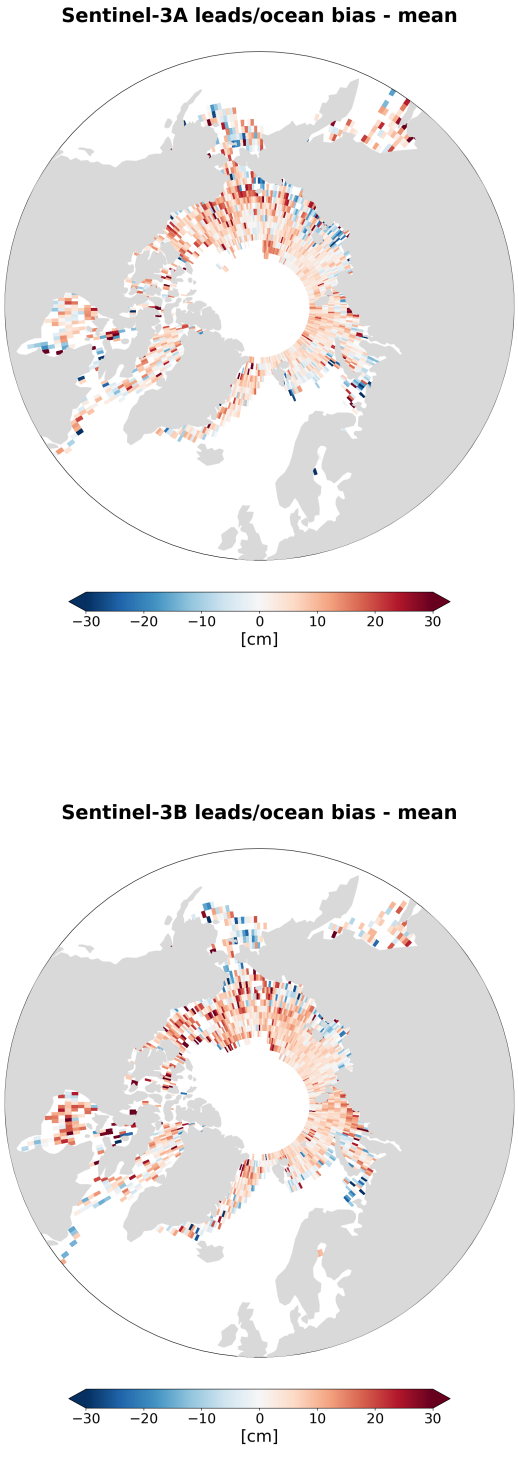

Figure 14: Map of open ocean/ice-covered SSHA differences for Sentinel-3A and Sentinel-3B in the Arctic ocean

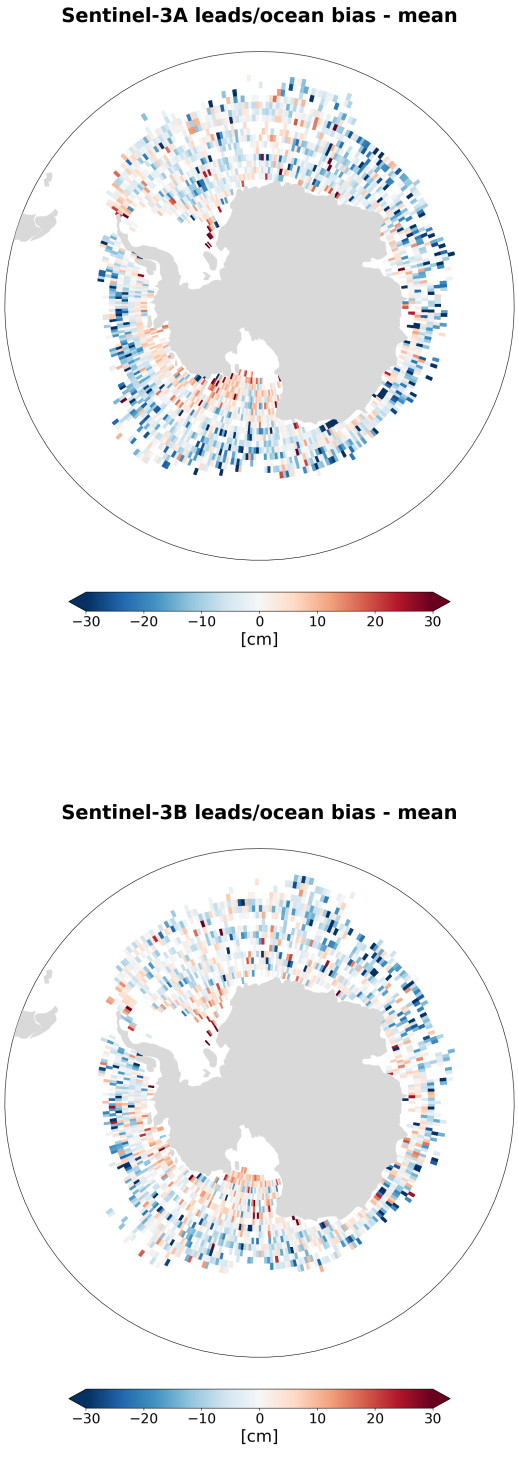

Figure 15: Map of open ocean/ice-covered SSHA differences for Sentinel-3A and Sentinel-3B in the Southern ocean

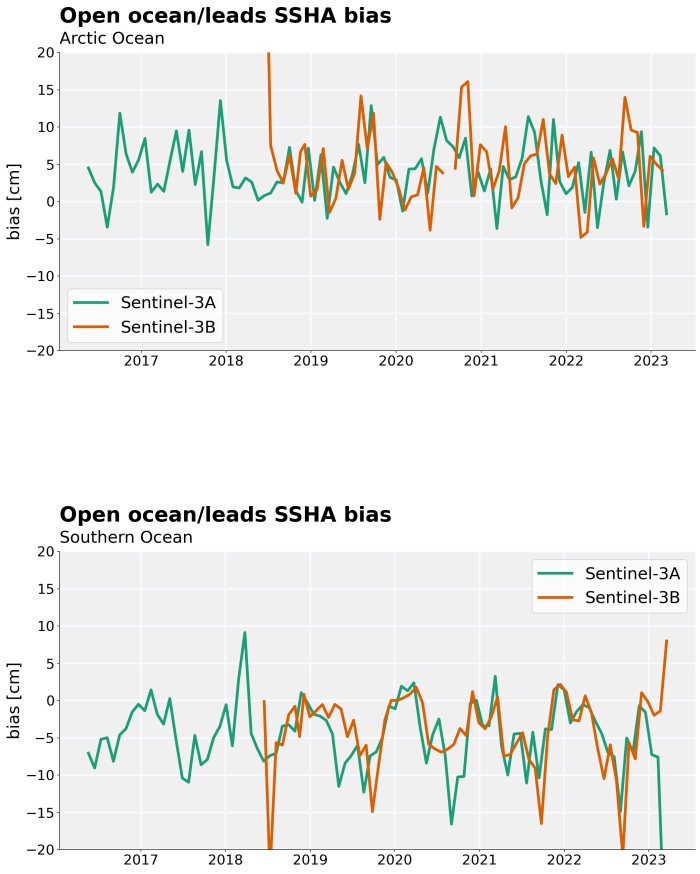

Figure 16: time series of open ocean/ice-covered SSHA differences for Sentinel-3A and Sentinel-3B in the Arctic and Southern oceans

3.4. Crossovers analysis

Figures 17 and 18 show maps of the mean and standard deviation of SSHA differences at Sentinel-3A/Sentinel-3A crossovers. Similar results are observed for Sentinel-3B/Sentinel-3B crossovers and not shown here. These analysis shows that, on average, there is an excellent consistency of Sentinel-3 missions. This is expected over ocean and remains true for SSHA estimations from leads (top panels of figures 17 and 18).

When considering the standard deviation of SSHA differences at xovers (bottom panels of figures 17 and 18), there is a rise in the standard deviation in ice-covered areas. This rise is more visible in the Arctic Ocean than in the Southern Ocean but maps of figures 17 and 18 integrate the whole period and mix open ocean and ice covered conditions.

To overcome this limitation, figure 19 separates open ocean and leads. Similar results are observed in the Arctic ocean (not shown). The separation of leads and open ocean illustrates higher noise levels in ice-covererd areas than in open ocean. Since higher natural ocean variability in ice covered areas is unlikely, it is probable that higher differences at crossovers results from higher error levels in leads. Errors can come from:

- errors in lead echo selection and/or processing,
- errors on one or several geophysical corrections (tide models for example are less accurate in the interior of the Arctic Ocean).

Estimates at crossovers presented here should not be compared directly to classical mission performance metrics derived from 1Hz data over ocean (with a typical standard deviation of SSHA differences of 5 cm) for two main reasons:

- crossovers presented here are based on high rate measurements and therefore have more high frequency content,
- over leads the measurements are non-uniformly distributed and the interpolation along ascending and descending tracks at the crossover location can be made over large distances, leading to potentially larger errors.

One example of a crossover in the ice covered Arctic Ocean is shown on figure 20 to illustrate the latter point.

Comparing Sentinel-3A and Sentinel-3B through crossovers shows that the consistency between missions is equivalent to the internal consistency of either Sentinel-3A or Sentinel-3B, as shown on figure 21 for the Arctic Ocean.

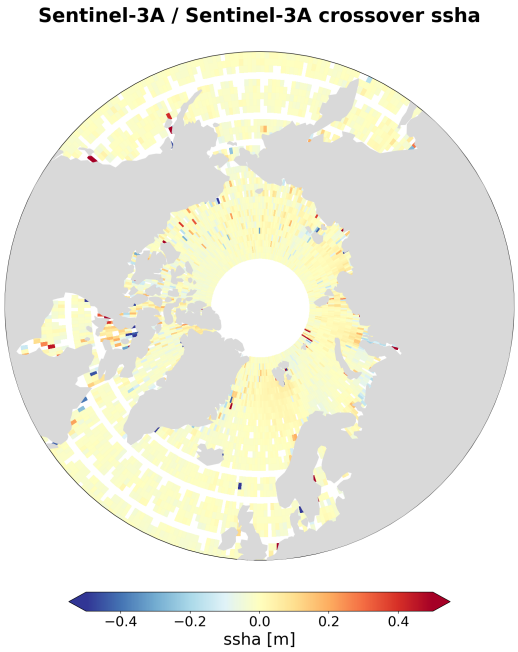

Figure 17: Maps of the mean (top) and standard deviation (bottom) of SSHA differences at crossovers in the Arctic Ocean for Sentinel-3A

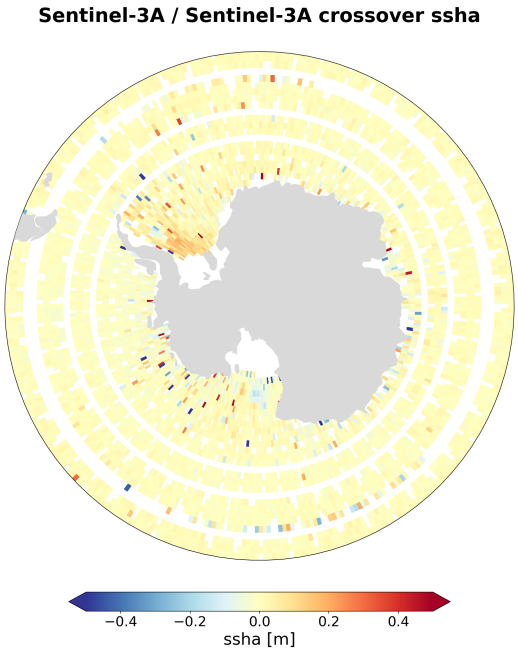

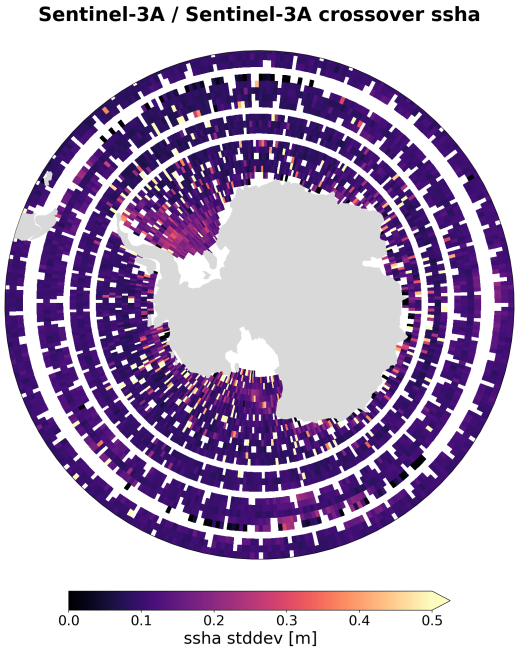

Figure 18: Maps of the mean (top) and standard deviation (bottom) of SSHA differences at crossovers in the Southern Ocean for Sentinel-3A

Figure 19: Maps of the standard deviation of SSHA differences at Sentinel-3A/Sentinel-3A crossovers in the Southern Ocean separating open ocean (top) and leads (bottom)

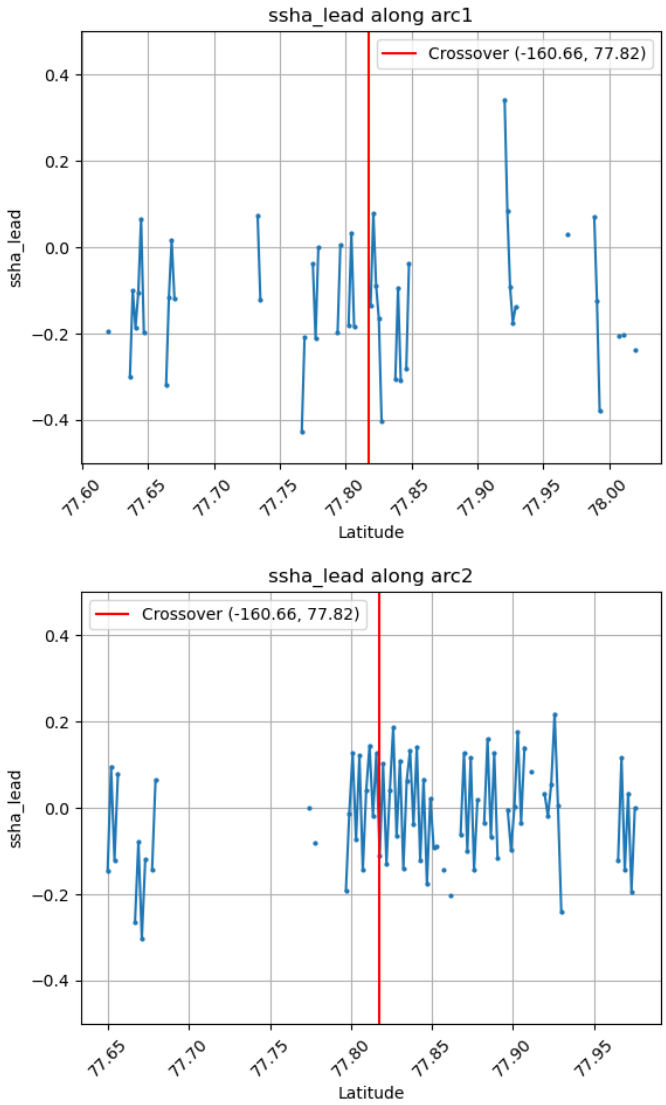

Figure 20: Example of one crossover in the ice-covered Arcitc ocean (red line) and sampling of leads SSHA along corresponding ascending and descending tracks

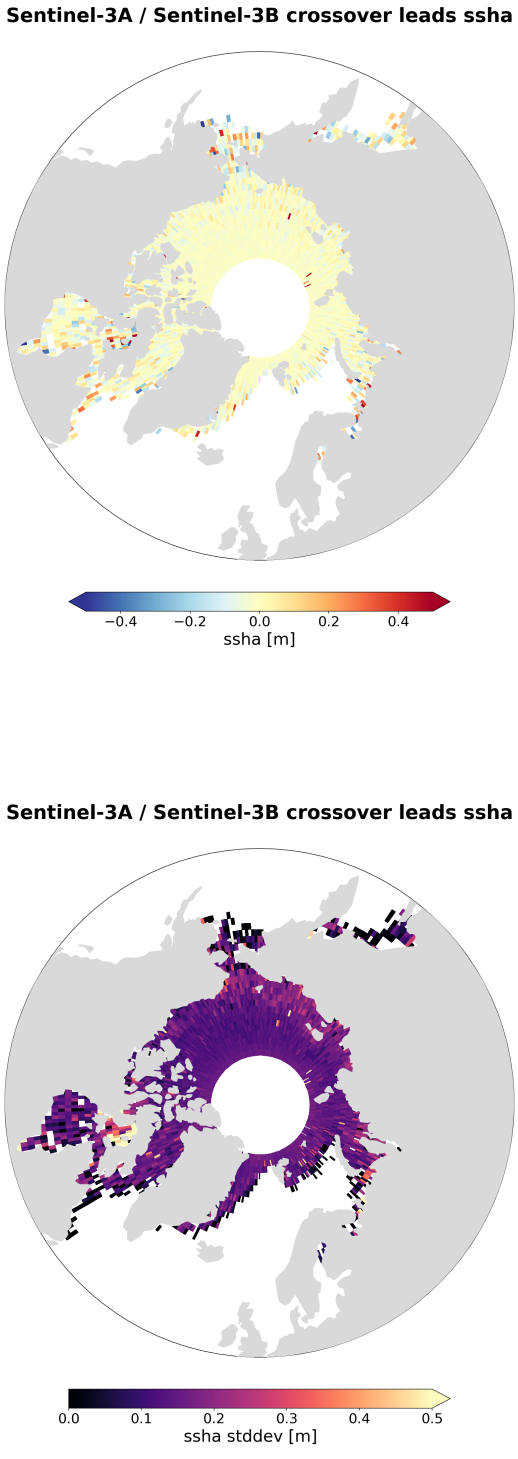

Figure 21: Maps of the mean (top) and standard deviation (bottom) of SSHA differences at Sentinel-3A/Sentinel-3B crossovers in the Arctic Ocean over leads.

4 Comparisons to other satellite altimetry datasets

This section provides a comparison of polar ocean sea level variability as observed by the Sentinel-3 mission with other satellite altimetry based products. Two other altimetry missions are used here, SARAL/AltiKa and CryoSat-2, chapter **2** describes the datasets used in the present analysis.

Results for the Arctic and Southern Oceans are very similar. We focus here on the Arctic Ocean where the CryoTempo product is available.

4.1. Observability

Figure 22 displays the ratio of SARAL/AltiKa measurements identified as leads in the Arctic Ocean. This should be compared to figure 3 for Sentinel-3. The geographical distribution of leads appears to be consistent between Sentinel-3 and SARAL/AltiKa. Computing the differences (figure 23) shows however that a larger share of echoes are identifed as leads by Sentinel-3A than by SARAL/AltiKa. In some large regions the ratio of echoes detected as leads is greater by about 10% on Sentinel-3 than on SARAL/AltiKa.

This is either coming from an over-detection on Sentinel-3 or an under-detection on SARAL/AltiKa. The SARAL/AltiKa algorithm used here is based on a neural network classifier of waveforms. This algorithm was validated against co-located SAR images [4]. In this paper, the authors also test a similar neural network based method on Sentinel-3A SARM echoes, with good results. The lead detection algorithm currently used on Sentinel-3 missions is based on pulse peakiness and sea-ice concentration.

Figure 22: ratio of leads measurements observed by SARAL/AltiKa in the Arctic Ocean

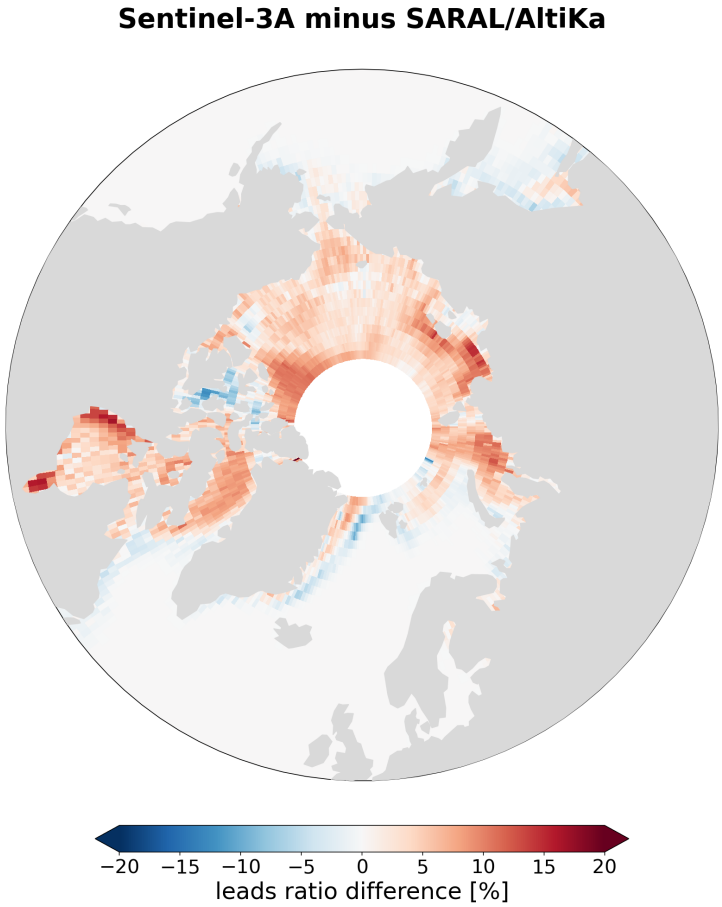

Figure 23: differences between the ratio of leads measurements observed by Sentinel-3A and SARAL/AltiKa in the Arctic Ocean

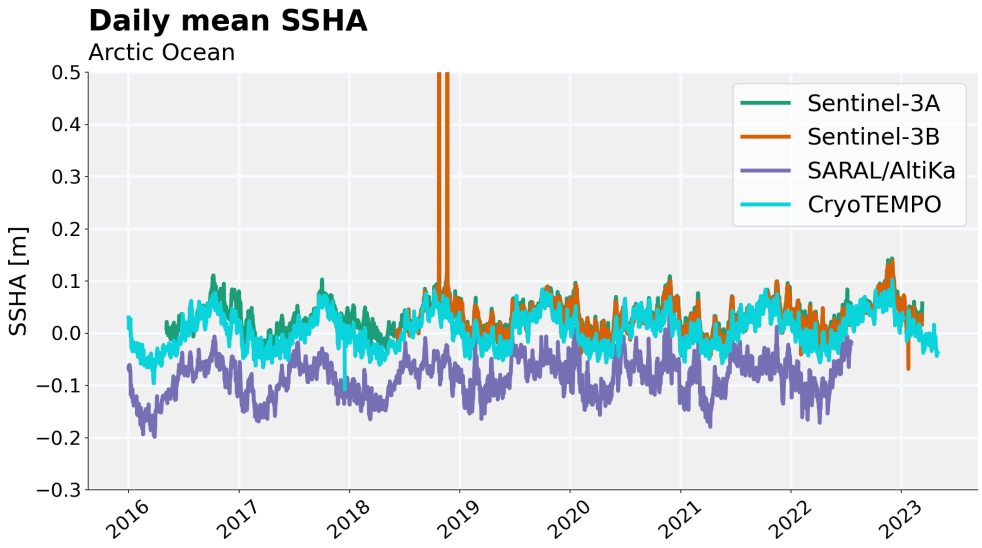

Figure 24: Arctic Ocean daily SSHA

4.2. SSHA variability

This section focuses on documenting the agreement and discrepancies of the Arctic ocean SSHA variability observed by Sentinel-3 compared to SARAL/AltiKa and Cryo-TEMPO data.

Figure 24 displays the daily mean SSHA in the Arctic Ocean from Sentinel-3A, Sentinel-3B, SARAL/AltiKa and Cryo-TEMPO. SARAL/AltiKa is offset by 10 cm but there is a good agreement at the regional level: no large drift is observed, seasonal signals agree well in terms of amplitudes and phases.

Figure 25 shows the mean SSHA from SARAL/AltiKa and Cryo-TEMPO data. These maps should be compared to the top panel of figure 8. Despite a mean bias (seen also on figure 24), SARAL/AltiKa and Cryo-TEMPO appear to be consistent.

Several differences are visible when compared to either Sentinel-3A or Sentinel-3B:

- a high along the eastern coast of Greenland is present on Sentinel-3, not on SARAL/AltiKa or Cryo-TEMPO
- SARAL/AltiKa and Cryo-TEMPO show a dipole pattern between the Beaufort Gyre and the Arctic interior. This is less visible on Sentinel-3 data.

Figure 26 shows the maps of the standard deviation of SSHA in the Arctic ocean from SARAL/AltiKa and Cryo-TEMPO data. These maps should be compared to figure 11 displaying the same quantity for Sentinel-3A. The difference is large here. While SARAL/AltiKa and Cryo-TEMPO show a drop in standard deviation in the Arctic interior, both Sentinel-3A (figure 11) and Sentinel-3B (not shown) display larger standard deviations in ice-covered areas than in the open ocean.

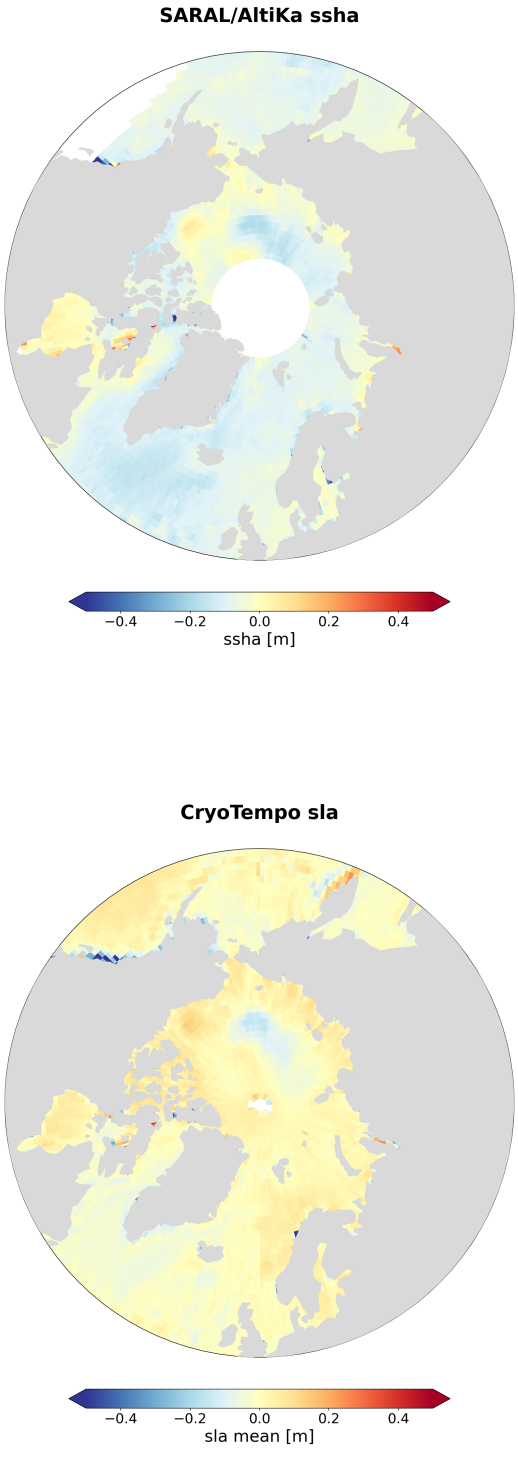

Figure 25: Maps of the mean SSHA in the Arctic Ocean from SARAL/AltiKa (top) and Cryo-TEMPO (bottom) data

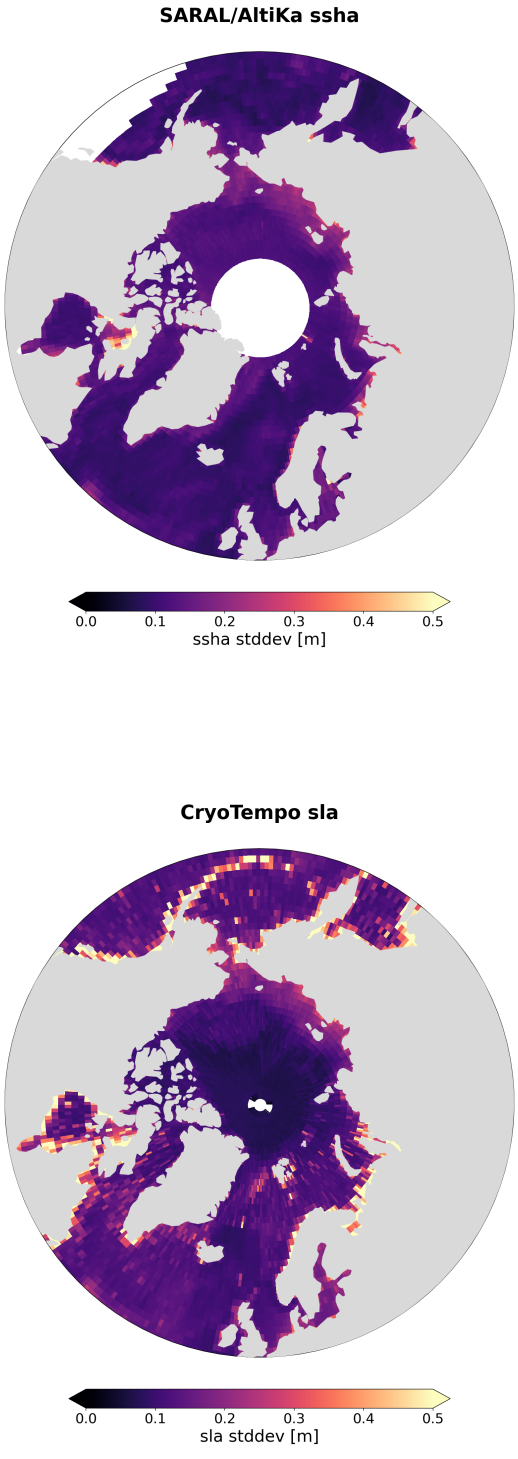

Figure 26: Maps of the standard deviation of SSHA in the Arctic Ocean from SARAL/AltiKa (top) and Cryo-TEMPO (bottom) data

5 Comparisons to in-situ measurements

This chapter provides comparisons between Sentinel-3 polar ocean topography measurements and in-situ measurements as a mean of qualitative validation. Finding in-situ data in permanently ice-covered regions is a challenge:

- the datasets are often affected by the harsh environment and limited maintenance capabilities, leading ot measurement gaps,
- they are often distributed with large delays,
- this is event more true in the Southern Ocean.

After reviewing available data, we provide here two comparisons between Sentinel-3 and in-situ stations. One is a bottom pressure recorder deployed in the Beaufort Gyre as part of the Beaufort Gyre Exploration Project (https://www2.whoi.edu/site/beaufortgyre/), deployed at 75°N and 210°E. Note that this is a bottom pressure recorder which does not measure steric height changes, while altimetry will.

The second one is a Japanese tide gauge at Syowa, along the coast of Antarctica (https://www.sonel.org/spip.php?page=maregraphe&idStation=2000), the data was retrieved from the University of Hawai'i Sea Level Center [2] and post processed to remove tidal and atmospheric effects.

This provides one comparison point in the central Arctic basin, and one in the Southern Ocean.

Time series of sea level variability from Sentinel-3A, Sentinel-3B and in-situ are shown on figures 27 for the Syowa tide gauge and 28 for the Beaufort Gyre data.

Unfortunately the Syowa tide gauge time series is not available after December 2021 and therefore does not overlap Sentinel-3 measurements over a long period. Qualitatively though the agreement is good: seasonal cycles amplitudes and phasing in agreement. Regarding both short (month to month) and long (interannual) variability, both the sampling provided by Sentinel-3 (27 days repeat cycle) and the limited time span make it hard to draw quantitative conclusions.

In the Arctic Ocean (figure 28), the seasonal signal in both altimetry and in-situ records is lower. Overall, variability levels are consistent between both in-situ and altimetry. Some signals seem to be well observed by altimetry like the large sea level drops in early 2017 and 2020.

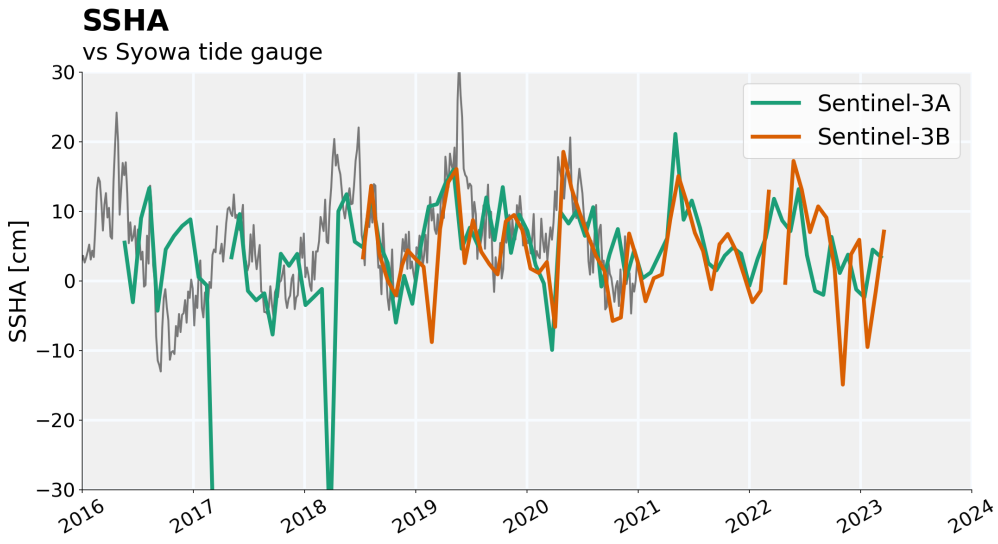

Figure 27: Sea level variations at Syowa tide gauge

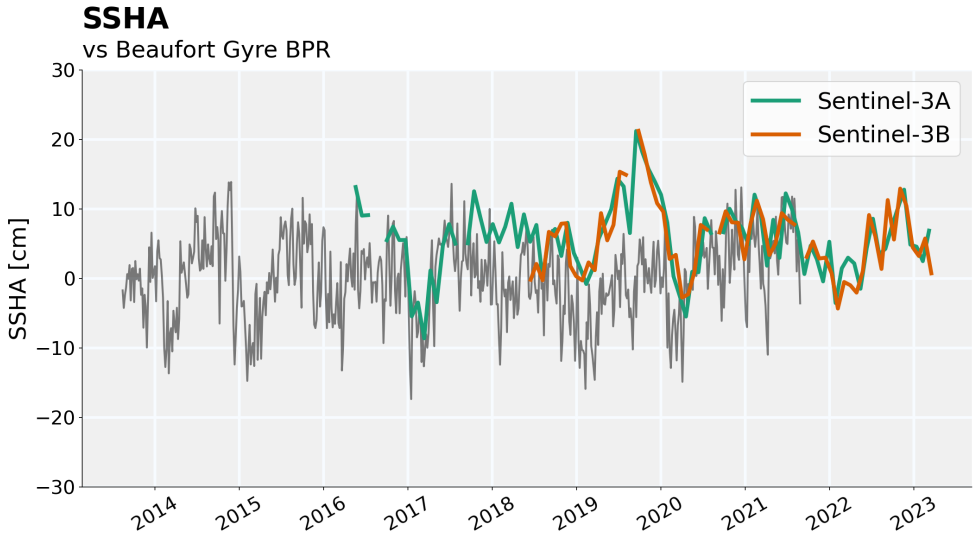

Figure 28: Sea level variations at the BGEP bottom pressure recorder

6 Conclusions

This report provides a synthetic view of Sentinel-3A and Sentinel-3B in polar oceans. It complements cyclic validation reports with long term monitoring metrics.

Below are several important findings:

- on average, and at large wavelengths Sentinel-3A and Sentinel-3B are able to observe ice-covered ocean SSHA variability, as shown when comparing basin-wide averages between missions or to in-situ measurments,
- however Sentinel-3A and Sentinel-3B exhibit a larger standard deviation of SSHA in the ice covered ocean compared to SARAL/AltiKa or Cryo-TEMPO data, indicating higher noise level,
- a residual ice-covered/open ocean bias is observed on Sentinel-3A and Sentinel-3B.

The higher noise level in the ice-covered parts of the ocean may be a result of different contributions. Among these contributions:

- errors in the waveform classification algorithm which is not severe enough, this would be compatible with the fact that the percentage of echoes classified as leads is lower on SARAL/AltiKa,
- less accurate geophysical and environmental corrections in polar regions, while we know that some corrections have higher error levels in the polar oceans, this should similarly impact SARAL/AltiKa and Cryo-TEMPO data,
- instrumental processing errors for peaky echoes from leads leading to higher high frequency variability level, for example jitter noise on non zero-padded echoes.

References

[1] Matthis Auger, Pierre Prandi, and Jean-Baptiste Sallée. Southern ocean sea level anomaly in the sea ice-covered sector from multimission satellite observations. *Scientific Data*, 9(1), March 2022. doi: 10.1038/s41597-022-01166-z. URL https://doi.org/10.1038/s41597-022-01166-z.

[2] Patrick C. Caldwell, Mark A. Merrifield, and Philip R. Thompson. Sea level measured by tide gauges from global oceans as part of the joint archive for sea level (jasl) since 1846, 2001. URL https://www.ncei.noaa.gov/archive/accession/JIMAR-JASL.

[3] Ghita Jettou, Manon Rousseau, Fanny Piras, Mathilde Simeon, and Ngan Tran. SARAL's full mission reprocessing: Improvement with the GDR-f standard. *Remote Sensing*, 15(10):2604, May 2023. doi: 10.3390/rs15102604. URL https://doi.org/10.3390/rs15102604.

[4] Nicolas Longépé, Pierre Thibaut, Rodolphe Vadaine, Jean-Christophe Poisson, Amandine Guillot, Francois Boy, Nicolas Picot, and Franck Borde. Comparative evaluation of sea ice lead detection based on sar imagery and altimeter data. *IEEE Transactions on Geoscience and Remote Sensing*, 57(6):4050–4061, 2019. doi: 10.1109/TGRS.2018.2889519.

[5] Pierre Prandi, Jean-Christophe Poisson, Yannice Faugère, Amandine Guillot, and Gérald Dibarboure. Arctic sea surface height maps from multi-altimeter combination. *Earth System Science Data*, 13 (12):5469–5482, November 2021. doi: 10.5194/essd-13-5469-2021. URL https://doi.org/10.5194/essd-13-5469-2021.